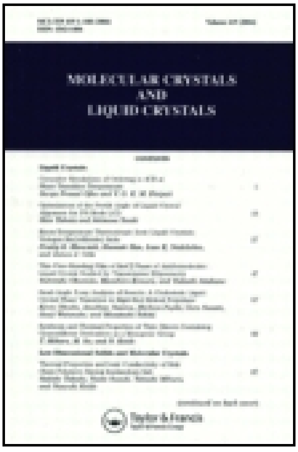

Molecular Crystals and Liquid Crystals Science and Technology. Section A. Molecular Crystals and Liquid Crystals

Publication details, including instructions for authors and subscription information:
http://www.tandfonline.com/loi/gmcl19

Time-Domain Optical Memory in Hole-Burning Materials

R. Kachru [a] , X. A. Shen [a] & Y. S. Bai [a]

[a] Molecular Physics Laboratory, SRI International, 333 Ravenswood Avenue, Menlo Park, CA, 94025, U.S.A.

Version of record first published: 24 Sep 2006.

To cite this article: R. Kachru , X. A. Shen & Y. S. Bai (1994): Time-Domain Optical Memory in Hole-Burning Materials, Molecular Crystals and Liquid Crystals Science and Technology. Section A. Molecular Crystals and Liquid Crystals, 252:1, 205-212

To link to this article: http://dx.doi.org/10.1080/10587259408038226

Mol. Cryst. Liq. Cryst. 1994, Vol. 252, pp. 205–212
Reprints available directly from the publisher
Photocopying permitted by license only

Printed in the United States of America

TIME-DOMAIN OPTICAL MEMORY IN HOLE-BURNING MATERIALS

R. Kachru, X. A. Shen, and Y. S. Bai
Molecular Physics Laboratory, SRI International, 333 Ravenswood Avenue, Menlo Park, CA 94025, U.S.A.

Abstract We have demonstrated storage of 2 Kbits of data at 40 Mbits/s in the Eu^{3+} doped Y_2SiO_5 crystal using the time-domain echo approach. Preventing coherent saturation, caused by the long data pulse train, is critical to the successful implementation of this technique. The experimentally inferred storage capacity of 6×10^4 spatial spot demonstrates the potential of this optical memory.

Keywords: hole-burning, photo-echo, optical memory

BACKGROUND

To illustrate the storage of information in the time domain using hole-burning materials, we use a simple diagram to describe the storage and retrieval of, first, a single bit, and then several bits, of information. Figure 1(a) shows the temporal sequence of laser pulses (i.e., the write, data, and read pulses) required to store and retrieve several bits of serial information. The frequency of the laser excitation pulses is fixed to a particular color that is in resonance with a particular group of atoms within the larger absorption line of the memory crystal. We use a rare-earth ion doped in a crystal as our memory crystal. At low temperatures (4 to 10 K), the width of the frequency absorption of a single rare-earth ion is very small (a few kilohertz). However, the overall absorption width of the memory crystal is much larger (many gigahertz) because the rare-earth ions occupy a distribution of different sites in a crystal. Therefore, individual ions do not see the write and data pulses occurring, respectively, at times $t_W = 0$ and t_D as two different pulses but rather as a complex pulse with a well-defined frequency Fourier transform.

For simplicity, Figure 1(b) shows the frequency Fourier transform (FT) of the write pulse and one of the data pulses from Figure 1(a). The FT of the three-pulse data pulse train shown in Figure 1(a) will be more complex than that shown in Figure 1(b). Figure 1(b) shows that the excitation spectrum is not uniform but is amplitude-modulated at frequencies proportional to the FT of the data pulse train.

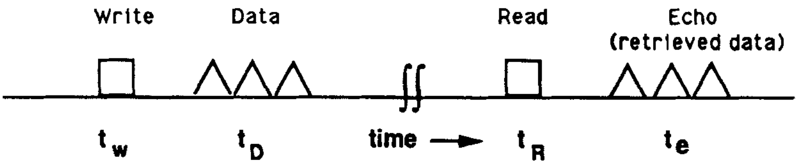

(a) Temporal sequence of laser pulses.

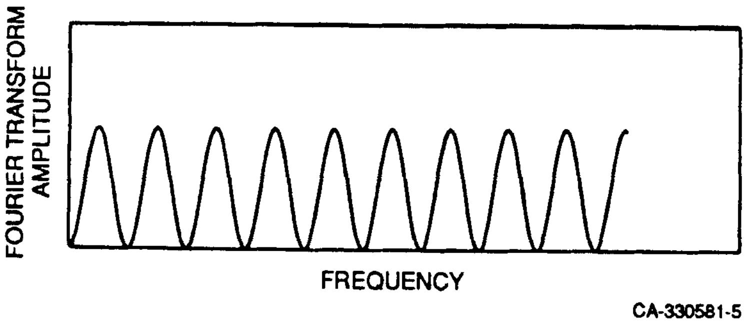

(b) Frequency Fourier transform of the write pulse and a single data pulse shown in (a)

FIGURE 1 Storage and retrieval of information.

Therefore, the absorption of the memory crystal around the color of the laser itself will be modulated as a function of the absorption frequency. In other words, within a micron-sized pixel in the memory crystal, the serial bits representing information in the time domain are stored by a small group of atoms absorbing a particular color of light by Fourier transforming the temporal signal into frequency-domain absorption modulation. The information can be stored for many hours at low temperatures.[1-5]

To read the information, we need only excite the memory crystal at time t_R with a single laser pulse of the same colors as the data and write pulses. The read pulse causes the atoms to take the inverse Fourier transform of the frequency population modulation, and the result is a coherent emission or stimulated echo (SE) by the memory crystal at time $t_R + (t_D - t_W)$. The echo pulse emitted by the memory crystal mimics the data pulse train, and the serial data can therefore be retrieved. Furthermore, the coherent nature of the emitted signal from the memory crystal allows the entire signal to be captured by a single detector at a high signal-to-noise ratio.

The potential storage density and read/write speeds for the stimulated echo memory can be evaluated by considering the restrictions placed on the laser pulses by the spectral properties of the absorbing atoms. The first requirement is that the laser pulses be separated by enough time that they are distinguishable. The minimum temporal separation between neighboring pulses is given by: $\tau_p = \frac{1}{\pi\delta_I}$, where δ_I (called the inhomogeneous linewidth) is the spread in the absorption frequencies of the atoms in the various sites in the sample.

The second requirement is that the last data pulse must arrive while the excited atomic dipoles can still compare it with the first data pulse. The maximum time between the first and last data pulse is given by: $T_2 = \frac{1}{\pi\delta_H}$ where δ_H (called the homogeneous linewidth) is the effective absorption linewidth of an atom at a specific site. T_2 is also called the dephasing lifetime. Its maximum value is the radiative lifetime of the excited state.

Thus, T_2/τ_p (or equivalently, δ_I/δ_H) bits of information at most can be stored in a single spot, and the read/write rate is just $1/\tau_p$. For Eu^{3+} doped in Y_2SiO_5, the optimum storage material, the ratio δ_I/δ_H is 5×10^6 and $\tau_p = 100$ ps, resulting in a read/write rate of greater than 10^{10} bits/s and a storage density of more than 10^6 bits per spatial spot.

In addition, the time-domain approach can be used for signal processing[6] and two-dimensional spatial image processing.[7]

TIME-FREQUENCY DOMAIN STORAGE

Because the SE memory can store 10^{12} bits/cm^3, its true potential can be realized by storing information not only in the time domain but also in the frequency domain of a single pixel in the memory crystal. For example, as shown in Figure 2, the entire absorption frequency of the memory crystal can be subdivided into N frequency bins (colors), each of which can store several bytes of serial information. This storage can be accomplished by using a narrow linewidth laser and setting its frequency (color) to the center of one bin. The pulse sequence shown in Figure 1(a) now stores and retrieves the serial information at this frequency bin within a pixel.

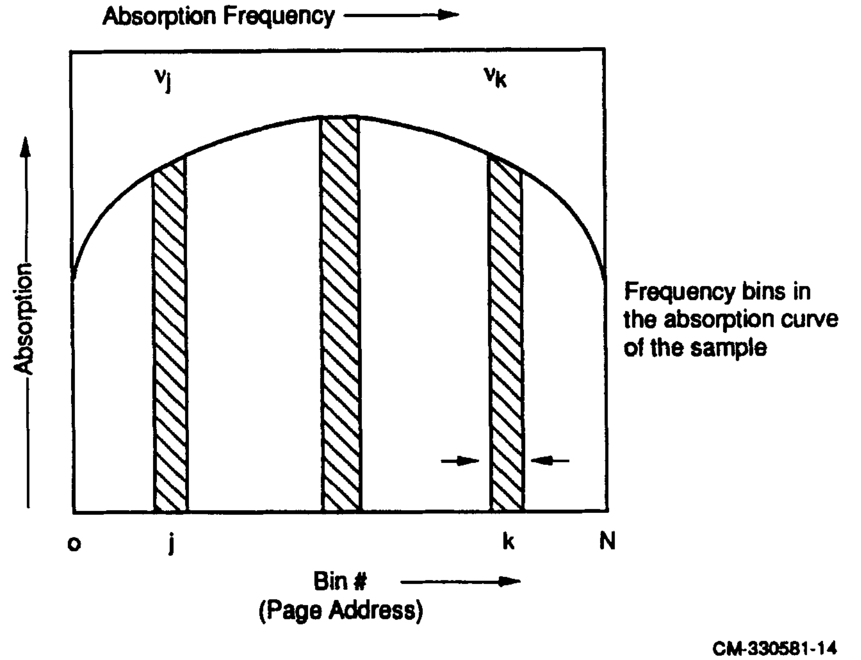

FIGURE 2 Division of absorption frequency spectrum into N frequency bins.

EXPERIMENTAL RESULTS

The experiment was performed on the 579.88-nm transition ($^7F_0$-$^5D_0$, site 1) of a 0.1% Eu^{3+}:Y_2SiO_5 crystal[8] at 2 K. The transition was found to have an inhomogeneous broadening of 3.6 GHz [full width at half maximum [FWHM of n(ν)], an optical density of 1.0 at the linecenter (l = 7.5 mm), and an oscillator strength of ~5×10^{-8}. The frequency of the laser (Coherent 699-21) was tuned to the side of the inhomogeneous line where the linear absorption is ~20%. The two-pulse echo dephasing time measured under these conditions with very weak input pulse energy flux was found to be ~800 μs.

The optical pulse sequence was generated by acousto-optically modulating the continuous-wave (cw) dye laser, with pulse 1 (3) as the write (read) pulse and pulse 2 the data, which is a binary-encoded pulse train with a rate of 40 Mbits/s. The laser pulses were focused onto the sample with a beam waist ($1/e^2$ intensity radius) of 80 μm and a power of 100 mW.

The Fourier transform of the echo signal is given by[3]

$$E_e(\omega) \propto E_1^*(\omega)\, E_2(\omega)\, E_3(\omega) \qquad (1)$$

where $E_k(\omega)$ is the electric field Fourier component of the k^{th} pulse.

Thus the echo will replicate pulse 2 (data) so far as the spectral product $E_1{}^*(\omega)$ $E_3(\omega)$ is approximately flat over the bandwidth of $E_2(\omega)$. This condition can be satisfied if pulses 1 and 3 are sufficiently short.[3] It can also be satisfied if pulses 1 and 3 are temporally long but identically frequency-chirped[9] so that their energy is evenly spread over the data bandwidth. Because the echo signal is proportional to the square of the write (read) pulse energy, the latter scheme is apparently more practical and thus was used in our experiment.

The frequency chirp was generated by ramping a VCO that drives the acousto-optical modulator (AOM) over a range of 44 MHz around the carrier RF f_0. The laser beam was double-passed through the AOM to compensate for the beam displacement associated with the frequency shift.[10] As a result, the effective chirp on the optical pulses was 88 MHz. The write and read pulses were of an identical duration (6 μs), which gave sufficient pulse area to generate large echo signals.

In order to avoid coherent saturation, the data pulse was phase-modulated by pseudorandom biphase shifting in addition to the amplitude modulation. The pseudorandom sequence generator is an 11-stage shift register (2047 bits) with an XNOR feedback and runs synchronously with the amplitude modulation of the data at 40 Mbits/s. The energy of the data was thus evenly distributed in the data bandwidth (80 MHz).

The echo signals were detected by an avalanche photodiode and recorded on a single-event basis by a digitizing oscilloscope. After each measurement, the laser was shifted by 110 MHz to a "fresh" spot. The power of the observed echo signal was about 0.01% that of the input data pulse when t_{32} (storage time) was shorter than the excited state lifetime (2 ms). Echo signals with large t_{32} were about 30 times smaller.

The results of a typical experiment with collinearly propagated pulses are shown in Figure 3. Figure 3(a) shows the input pulse sequence and the echo signal (retrieved data) for a 10-μs data pulse (400 bits). The input pulses are attenuated by ~10^{-4}. Figure 3(b) shows pulse 2 (input data) on an expanded time scale, and Figure 2(c) shows the retrieved data on an expanded time scale. Figure 3(d) shows the same data retrieved (with P_1 and P_2 off) after ~2 minutes. The signal was amplified by a factor of 26. No noticeable signal degradation was observed after reading was repeated up to 10 times.

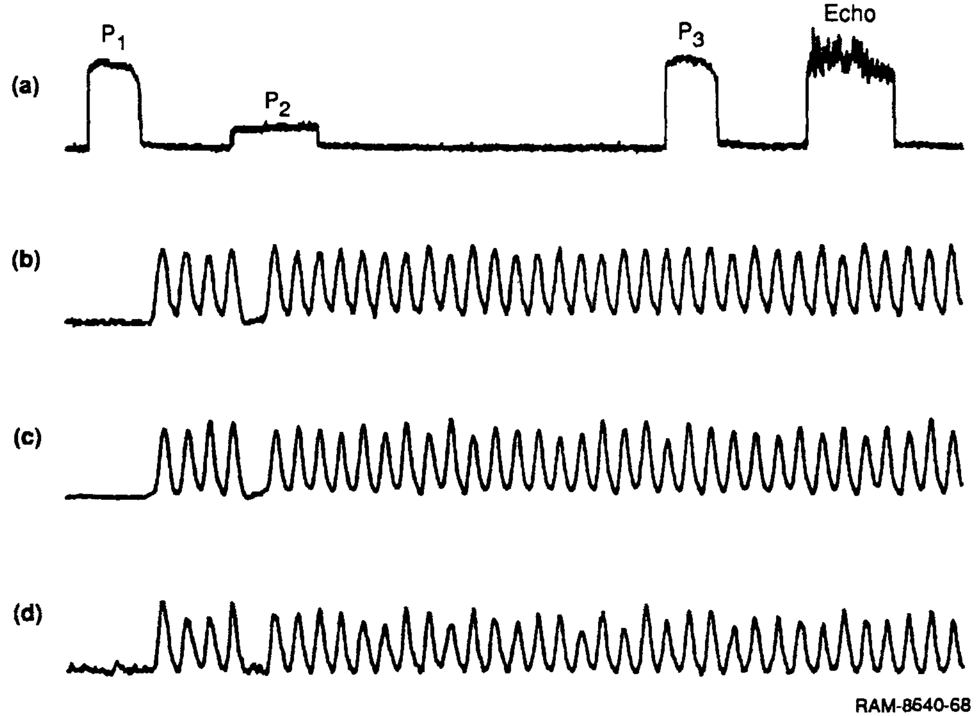

FIGURE 3 Results of a typical experiment with collinearly propagated pulses. a) Input pulse sequence and echo signal. Full horizontal scale = 102.4 μs. The duration of the data pulse is 10 μs (400 bits). The input pulses are attenuated by ~10^{-4}. b) Input data pulse (P_2) on an expanded time scale. Full horizontal scale = 2 .4 μs. c) Retrieved data pulse (echo) on an expanded time scale. d) The same data retrieved (with P1 and P2 off) after ~2 minutes. The signal was amplified by a factor of 26.

In Figure 4, we show the storage and retrieval of a 2-kbit data package (total duration = 50 μs). Figure 4(a) shows the beginning portion of the input data pulse train, Fig 4(b) shows the retrieved data package at t_{32} = 100 μs, Figure 4(c) shows the retrieved data at t_{32} = 2.2 ms.

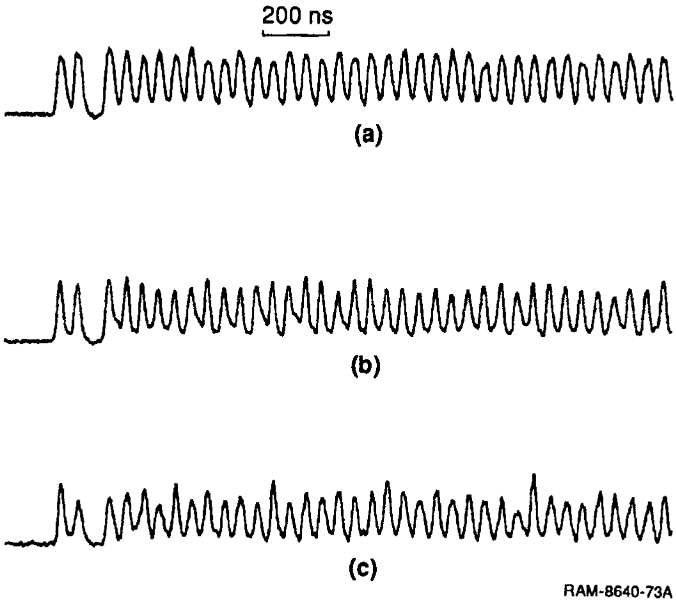

FIGURE 4 Storage and retrieval of 2 Kbit/spot data. (a) Beginning portion of the input data pulse stream, (b) initial portion retrieved data at t_{32} = 100 μs and (c) initial portion of data retrieved at t_{32} = 2.2 ms.

As mentioned earlier, the separation between the frequency channels used in this experiment was 110 MHz and the inhomogeneous width of the transition was 3.6 GHz. About 32 frequency channels should, in principle, be available on this transition. Thus the inferred storage capacity from this experiment is $> 6.25 \times 10^4$ bits per spatial spot. Taking into account the total excitation volume, we find that the storage density obtained here is 4×10^8 bits/cm^3.

Our reason for working with a very low absorption ($\alpha\ell \sim 0.25$) in this experiment was to minimize the excitation-induced dephasing. As has been shown, the excitation-induced dephasing is proportional to the absorption coefficient α and independent of the sample length ℓ. On the other hand, it is known[11] that the echo efficiency is maximized at $\alpha\ell \sim 1$. In fact, echo efficiency at least 10 times as high as obtained in our experiment is routinely observed in most stimulated echo experiments when this condition is satisfied. It is conceivable that we can get similar efficiency with a longer crystal (ℓ = 30 mm). In addition, the signal detectability was limited by the noise of our amplifier, which can be improved by a factor of 10. Taking into account these two factors, we could reduce the laser beam waist to 8 μm and the input power to 1 mW and still obtain a similar signal-to-noise ratio. The volume storage density thus calculated is 0.8×10^{10} /cm^3, which sets the lower limit that can be obtained with existing technology. The corresponding two-dimensional storage density is 2.4×10^{10} /cm^2, which is about 3 orders of magnitude higher than that of compact discs.

CONCLUSIONS

We have experimentally determined the realistic limits of data storage density, speed, compactness, and signal-to-noise ratio when existing materials and technology are used. We have shown that the storage density approaches the theoretical limit at a competitive input/output speed. To achieve this breakthrough, we have investigated the coherent saturation problem and discovered techniques that circumvent it. We believe that our results conclusively suggest time domain hole burning memory is practically viable.

ACKNOWLEDGEMENTS

This research was supported by U.S. Air Force Office of Scientific Research.

REFERENCES

1. T. W. Mossberg, A. Flussberg, R. Kachru, and S. R. Hartmann, Phys. Rev. Lett. 42, 1665 (1979).
2. R. Kachru, T. W. Mossberg, and S. R. Hartmann, Opt. Commun., 30, 57 (1979).
3. T. W. Mossberg, Opt. Lett., 7, 77 (1982).
4. N. W. Carlson, W. R. Babbitt, and T. W. Mossberg, Opt. Lett., 8, 623 (1983).
5. M. K. Kim and R. Kachru, J. Opt. Soc. Am., 134, 305 (1987).
6. X. A. Shen, Y. S. Bai, and R. Kachru, Opt. Lett., 17, 1079 (1992).
7. X. A. Shen and R. Kachru, Opt. Lett., 17, 520 (1992).
8. R. Yano, M. Mitsunaga, and N. Uesugi, Opt. Lett., 16, 1884 (1991); M. Mitsunaga, R. Yano, and N. Uesugi, Opt. Lett., 16, 1890 (1991).
9. Y. S. Bai, W. R. Babbitt, and T. W. Mossberg, Opt. Lett., 11, 724 (1986).
10. Y. S. Bai and R. Kachru, Opt. Lett. 14, 1189 (1993).
11. R. Friedberg and S. R. Hartmann, Phys. Lett., 37A, 285 (1971).